

# Transport calculation of dilepton production at ultrarelativistic energies

C. Ernst<sup>a</sup>, S. A. Bass<sup>b</sup>, S. Soff<sup>a</sup>, H. Stöcker<sup>a</sup> and W. Greiner<sup>a</sup>

<sup>a</sup>*Institute for Theoretical Physics, University of Frankfurt, Robert-Mayer-Strasse 8-10, D-60054 Frankfurt, Germany*

<sup>b</sup>*Department of Physics, Duke University, Durham, North Carolina 27708-0305, USA*

## Abstract

Dilepton spectra are calculated within the microscopic transport model UrQMD and compared to data from the CERES experiment. The invariant mass spectra in the mass region between 300 and 600 MeV depend strongly on the mass dependence of the  $\rho$  meson decay width which is not sufficiently determined by the Vector Meson Dominance (VMD) model. A consistent explanation of both the recent Pb+Au data and the proton induced data can be given without additional medium effects.

## I. INTRODUCTION

Recently, electromagnetic radiation in form of lepton pairs has been observed at CERN in the CERES experiment. A strong enhancement above the cocktail of hadronic decays has been reported. This is interesting, because dileptons may escape nearly undisturbed from the hot and dense zone which is formed in the heavy ion collision. Dileptons could probe the intermediate stage of these interactions. On the other hand, hadrons are thought to probe the later freeze-out stages. This folklore may not be entirely correct: A number of investigations indicate that hadronic signals such as strangeness and entropy, as well as flow are developed in the early phase, while a large fraction of the observed dileptons is simply due to post-freeze-out decays ("feeding") of isolated hadrons.

The fact that also dileptons are emitted from various sources and during the entire reaction makes the interpretation of this signal not as easy as hoped for. Electromagnetic probes are definitely not a pure signal from the most interesting high density stage only! Rather, their spectrum is composed of different contributions integrated over the full interaction dynamics. Transport models need to be applied to decompose the dilepton cocktail into its various individual contributions.

The most discussed feature of the data is the enhancement of intermediate mass lepton pairs ( $300 \text{ MeV} < M_{ee} < 700 \text{ MeV}$ ) as compared to the hadronic cocktails based on primary collisions. While the enhancement at BEVALAC energies is still not understood [1–4], first predictions for Pb+Au collisions from transport models including secondary production of dileptons (e.g.  $\pi\pi \rightarrow e^+e^-$ ) indicated only a small (if any) deviation from the CERES data

[5,6]. A large variety of attempts has been made to explain this deviation. The two most popular of them are the hypothesis of lowering vector meson masses (the Brown-Rho scaling) [7–9] and the collisional broadening of the spectral functions in the hadronic environment [10,11].

Here we analyse the recent CERES data on the multiplicity and  $p_t$  of the lepton pairs. First, we give a survey of the dilepton production in the framework of the ultrarelativistic quantum molecular dynamics model, UrQMD [12]. The present paper demonstrates that a state-of-the-art transport model based on hadronic and string degrees of freedom can predict the present data without assuming phase transitions or unconventional in-medium effects. This compares well to recent results from a simple transport model [13].

## II. DESCRIPTION OF THE MODEL

Dilepton production in the framework of the UrQMD model has been considered in some detail in ref. [4]. In this model dileptons are produced perturbatively, mainly in hadronic decays. Dalitz decays of neutral mesons and direct decays of vector mesons are taken into account. The incoherently summed  $pn$  bremsstrahlung as well as the  $\Delta(1232)$  Dalitz decay are of minor importance at CERES energies because the system is dominated by mesonic degrees of freedom. All dilepton decay widths have been specified in [4].

For the vector meson decay width  $\Gamma_{\rho \rightarrow e^+e^-}(M)$  we use the typical  $M^{-3}$  dependence which results from vector meson dominance (VMD model). There seems to be some inconsistency between the original formulation of VMD (see e.g. Sakurai [14]), which results in a  $M^{-3}$  dependence for  $\Gamma_{\rho \rightarrow e^+e^-}$  and the extended VMD from Kroll, Lee and Zumino [15] implying a dilepton decay width proportional to  $M$  (see e.g. ref. [16]). The discrepancy between these two approaches seems to be as  $M^4$ ! However, if one considers the channel  $\pi\pi \rightarrow e^+e^-$ , the extended VMD requires also a direct coupling between the electromagnetic and the hadronic channel. If this term is included (as well as the interference), one ends up with the overall  $M^{-3}$  dependence again.

In the extended VMD the direct term can be motivated only by a  $\pi\pi\gamma$  coupling. Therefore it is not clear how to treat the dilepton decay of  $\rho$  mesons which themselves come from heavy resonance decays or even string fragmentation. Similar problems arise for the  $\omega$  and  $\phi$  decays. However, due to their small total widths, this effect does not manifest itself in the dilepton mass spectra and is thus not discussed separately here. In the UrQMD model the following procedure is applied:

For  $\rho$  mesons which are produced by  $\pi\pi$ -annihilations or in decays of baryonic or mesonic resonances the dilepton decay width scales like  $M^{-3}$ . The dilepton width for  $\rho$  mesons from string fragmentation is chosen according to the direct term of the extended VMD model which scales like  $M$ . Other approaches are possible and yield different results: see discussion below.

## III. RESULTS

The undisturbed dilepton mass spectrum for proton on beryllium collisions at 450 GeV incident energy is shown in fig. 1. This 'naked' spectrum could be verified only with an ideal

detector covering the  $4\pi$  phase space angle and having a perfect momentum resolution (the bin width is 8 MeV). It shows all details of the model calculation. The CERES data [17] are drawn for orientation only and should not be directly compared to the actual calculation. One sees, however, that roughly two orders of magnitude are lost due to the acceptance.

At low invariant masses the overwhelming background is due to the Dalitz decays of the long-living mesons  $\pi^0$  and  $\eta$ . Between 500 and 750 MeV the  $\omega$  Dalitz and the direct  $\rho$  meson decays dominate the spectrum. At higher energies the characteristic peaks of the direct  $\omega$  and  $\phi$  decays overlap the  $\rho$  decay. The  $\eta'$  Dalitz decay or baryonic channels like  $pn$  bremsstrahlung play only a subordinate role. The asymmetrical shape of the  $\rho$  mass distribution is due to phase space limitations and especially due to the  $M^{-3}$  scaling of the decay width. At invariant masses around 1.2 GeV there is a drop in the  $\rho$  distribution. This is due to a limitation of the model not to create resonances from string fragmentation with masses exceeding the pole mass more than three widths ( $M < M_R + 3\Gamma_R$ ).

For comparison with the experimental data from the CERES collaboration, one needs to correct the model calculations for the limited detector acceptance and momentum resolution. Because the detector covers only a small geometric region, every detected particle must have a certain angle to the beam axis. This requires the pseudo rapidity of the lepton  $\eta_{e^\pm}$  to be  $2.1 \leq \eta_{e^\pm} \leq 2.65$ . A cut on small opening angles  $\Theta_{e^+e^-} > 0.035$  mrad of the electron-positron pair has to be matched because close pairs cannot be identified by the RICH detectors. The individual leptons which have passed the initial RICH detectors are then deflected in a magnetic field with a momentum resolution parameterised as

$$\frac{\Delta p}{p} = \sqrt{\alpha^2 + (\beta p)^2}, \quad (1)$$

where  $\alpha$  and  $\beta$  depend on the detector setup and are listed in table 1 [18]. The momenta of the electron and positron are washed out accordingly with a Gaussian distribution function of width  $\frac{\Delta p}{p}$ . Finally, these tracks have to survive a transverse momentum cut, which is typically  $p_t > 50$  MeV for the proton induced and  $p_t > 200$  MeV for the ion induced reactions.

In fig. 2 we present the dilepton mass spectra for proton on beryllium collisions including the CERES acceptance and resolution. As compared to fig. 1 the momentum resolution has washed out the peak structures and the low mass pairs have been suppressed due to the acceptance. As an effect of the finite resolution one can see also contributions from the direct  $\rho^0$  decay below the two pion threshold. The transport calculation slightly overestimates the data around the vector meson poles but seems to be consistent with the overall data set. At invariant masses higher than 1.3 GeV the data possibly indicate a need for additional sources like direct production in meson+meson collisions (see e.g. [19]) which were not considered in the present calculation.

The UrQMD result for the heaviest system measured by CERES can be found in fig. 3 together with the data from the '96 run [18]. These default calculations do not show the typical trend to underestimate the data in the region around 400 MeV. Like in a number of other free or conventional transport calculations the data point at 780 MeV, just at the  $\rho/\omega$  mass, is slightly overestimated [10,11,13]. This has been interpreted that 'some of the signal should be distributed away' by medium effects. However, in view of the good agreement of the conventional calculation at lower masses one must ask, where this strength should

go. Furthermore, we have observed that introducing collision widths results in a significant enhancement of vector meson production, which is not compatible to the data.

Two data points are missed at 140 MeV and 180 MeV. By lowering the  $p_t$  cut to less than 200 MeV this dip can be artificially removed on cost of overshooting the data points at 63 MeV and 88 MeV. Our interpretation of this observation is that the UrQMD  $p_t$ -distribution of pions and etas is too soft to be compatible to this data. Furthermore the spectral density of the  $\rho$  meson in nuclear matter might extend to below  $2m_\pi$  because the  $\rho$  may decay into a nucleon nucleon-hole pair. This contribution is neglected in all on-shell transport models like UrQMD, but might fill in this gap.

The results of the transport simulation depend on the details of the VMD model (fig. 4). In the default calculation, the dilepton decay width of  $\rho$  mesons scales like  $M^{-3}$  if they are from hadronic sources and like  $M$  for  $\rho$ 's from strings (see the discussion above). If no VMD was considered at all, i.e. assuming constant dilepton decay widths for the  $\rho$ , a clear enhancement of the data over the model calculation can be observed (dashed line in fig. 4). However, as pointed out above, neglecting the  $M^{-3}$ -dependence of the  $\rho$  meson dilepton decay width is not a valid assumption. In the hydrodynamical calculations of ref. [20] the  $M^{-3}$  factor is missed, which might be the reason for their underestimation of the CERES data.

On the other hand, one can assume 'total VDM' by requiring that the vector mesons which were produced in string fragmentation scale like the 'hadronic'  $\rho$ 's with  $M^{-3}$ . This leads to an overestimation of the Pb+Au data (see dotted line in fig. 4) and also the p+Be data are overestimated. From a theoretical point of view this approach has to be considered as an upper limit to the contribution of dilepton emission from  $\rho$  mesons from string fragmentation. Contrary, the default calculation provides a lower limit for a realistic dilepton spectrum. The range between both approaches is the result of our uncertainty how to treat dilepton production from string fragmentation.

The recent lead data have also been analysed for the transverse momenta of the lepton pairs (i.e. the virtual photons). The idea was to cut on pairs emitted from low- $p_t$  vector mesons for which the interaction with the surrounding medium should be strongest. Consequently, in-medium effects would result in a stronger enhancement of the low- $p_t$  data set over conventional models. The results of the corresponding UrQMD analysis are shown in fig. 5 in comparison to the CERES data [18].

Note, first of all that the dip below  $M_{e^+e^-} = 200$  MeV which was already observed in fig. 3 can be found only in the high  $p_t$  region (lower frame). This indicates once more that UrQMD predicts less high- $p_t$   $\pi^0$  and  $\eta$  mesons.

In the  $\rho$  region a reasonable agreement between simulation and data can be found both for the low- $p_t$  (upper frame) and the high- $p_t$  sample. In particular the low- $p_t$  data are consistent with the present UrQMD calculation – without a need for additional medium effects.

#### IV. CONCLUSION

In summary, the p+Be and the Pb+Au CERES data can be consistently explained by the UrQMD transport simulations. A reasonably good agreement was found especially in the region of  $0.3 \text{ GeV} < M < 0.6 \text{ GeV}$ . It was discussed that the parameterisation of the vector

meson decay width is not constrained from first principles. The variation between different approaches for  $\Gamma_{\rho \rightarrow e^+e^-}(M)$  manifests itself in dilepton spectra clearly underestimating or slightly overshooting the CERES data. Further efforts in theory are required to provide a microscopic scheme for  $\Gamma_{\rho \rightarrow e^+e^-}(M)$ . Measurements with higher precision could help to identify the  $\omega$  peak in the invariant mass spectra and thus pin down the shape of the  $\rho$  meson. In addition more experimental information on the elementary channels  $p+p$ ,  $\pi+p$ , especially a separate measurement of the Dalitz contribution (e. g. with TAPS), could be used to verify the different realisations of the VMD.

### ACKNOWLEDGMENTS

The authors want to thank W. Cassing, B. Friman and J. Knoll for helpful discussions. This work was supported in parts by Graduiertenkolleg Theoretische und Experimentelle Schwerionenphysik, GSI, BMBF, DFG, J. Buchmann Foundation, A. v. Humboldt Foundation and D. O. E. grant DE-FG02-96ER40945.

## REFERENCES

- [1] R. J. Porter *et al.*, Phys. Rev. Lett. **79**, 1229 (1997).
- [2] E. L. Bratkovskaya, W. Cassing, R. Rapp, and J. Wambach, Nucl. Phys. **A634**, 168 (1998).
- [3] E. L. Bratkovskaya and C. M. Ko, Phys. Lett. **B445**, 265 (1999).
- [4] C. Ernst, S. A. Bass, M. Belkacem, H. Stöcker, and W. Greiner, Phys.Rev. **C58**, 447 (1998).
- [5] L. A. Winckelmann, S. A. Bass, M. Bleicher, M. Brandstetter, C. Ernst, L. Gerland, J. Konopka, S. Soff, C. Spieles, H. Weber, C. Hartnack, J. Aichelin, N. Amelin, H. Stöcker, and W. Greiner, Nucl. Phys. **A610**, 116c (1996).
- [6] V. Koch and C. Song, Phys. Rev. **C54**, 1903 (1996).
- [7] G. E. Brown and M. Rho, Phys. Rev. Lett. **66**, 2720 (1991).
- [8] T. Hatsuda and S. H. Lee, Phys. Rev. **C46**, R34 (1992).
- [9] G. Q. Li, C. M. Ko, G. E. Brown, and H. Sorge, Nucl. Phys. **A611**, 539 (1996).
- [10] R. Rapp, G. Chanfray, and J. Wambach, Nucl. Phys. **A617**, 472 (1997).
- [11] W. Cassing, E. L. Bratkovskaya, R. Rapp, and J. Wambach, Phys. Rev. **C57**, 916 (1998).
- [12] S.A. Bass, M. Belkacem, M. Bleicher, M. Brandstetter, L. Bravina, C. Ernst, L. Gerland, M. Hofmann, S. Hofmann, J. Konopka, G. Mao, L. Neise, S. Soff, C. Spieles, H. Weber, L.A. Winckelmann, H. Stöcker, W. Greiner, C. Hartnack, J. Aichelin, N. Amelin, *Prog. Part. Nucl. Phys.* **41** 255 (1998).
- [13] V. Koch, (1999), nucl-th/9903008.
- [14] J. J. Sakurai, *Currents and fields*, 1. ed. (Chicago Univ. Press, Chicago, 1969).
- [15] N. M. Kroll, T. D. Lee, and B. Zumino, Phys. Rev. **157**, 1376 (1967).
- [16] F. Klingl, N. Kaiser, and W. Weise, Z. Phys. **A356**, 193 (1996).
- [17] G. Agakishiev *et al.*, Europ. Phys. J. **C4**, 231 (1997).
- [18] B. Lenkeit, Phd thesis, Heidelberg (1998) and private communication
- [19] G. Q. Li and C. Gale, Phys. Rev. **C58**, 2914 (1998).
- [20] J. Sollfrank *et al.*, Phys. Rev. **C55**, 392 (1997).

TABLES

	$\alpha$	$\beta \text{ (MeV)}^{-1}$
p + Be (1994)	0.043	0.053
Pb + Au (1996)	0.035	0.023

TABLE I. Parameters of the CERES momentum resolution (see text).

## FIGURES

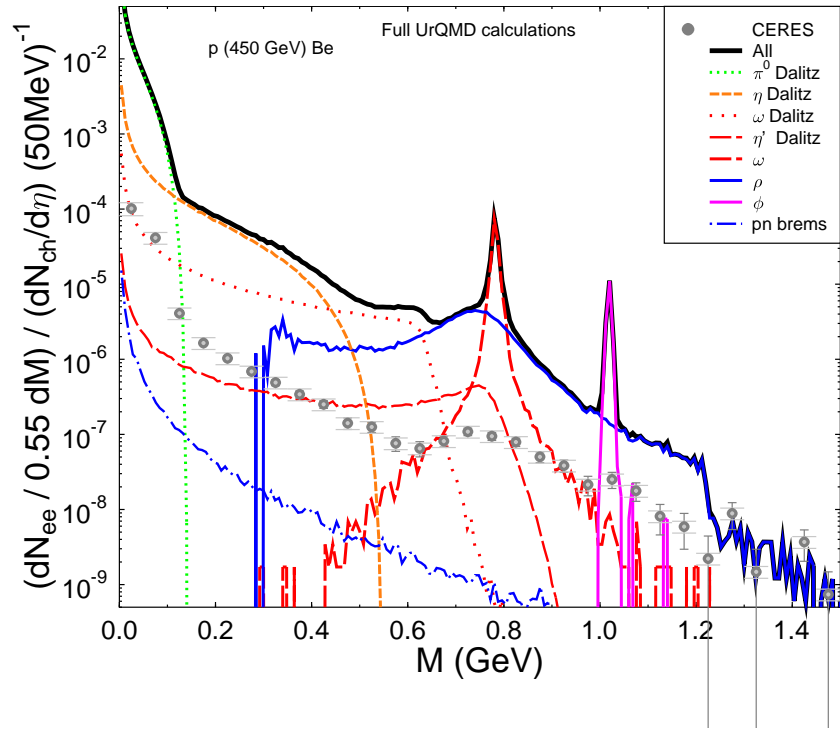


**Fig. 1** 'Ideal' dilepton spectrum of  $p + \text{Be}$  collisions at 450 GeV. The UrQMD results are not filtered and the data points are for orientation only.



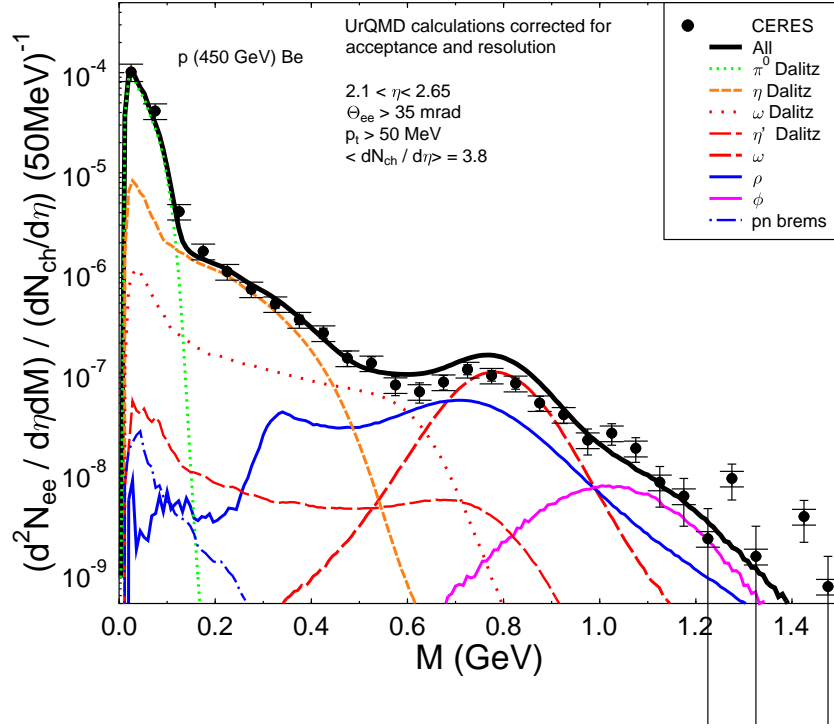


**Fig. 2** Dilepton spectrum of p + Be collisions at 450 GeV. UrQMD calculation, corrected for acceptance and resolution, in comparison to data [17]

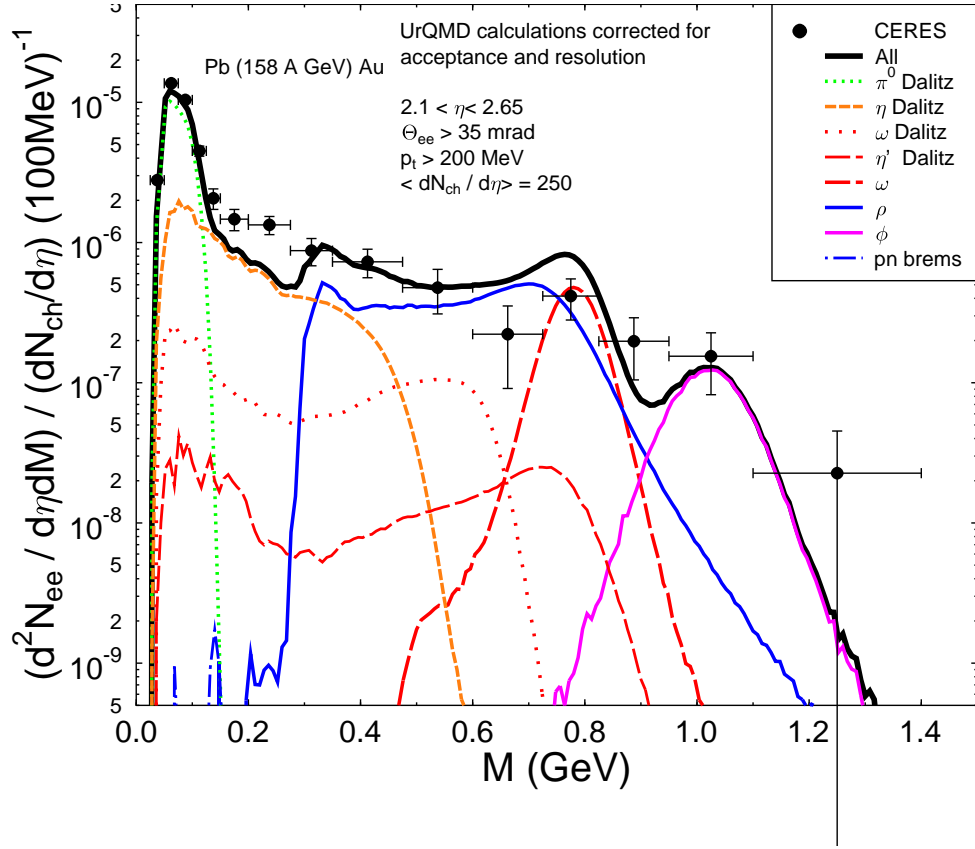


**Fig. 3** Dilepton spectrum of Pb + Au collisions at 158 A GeV. The '96 CERES data [18] compared to filtered UrQMD calculations.

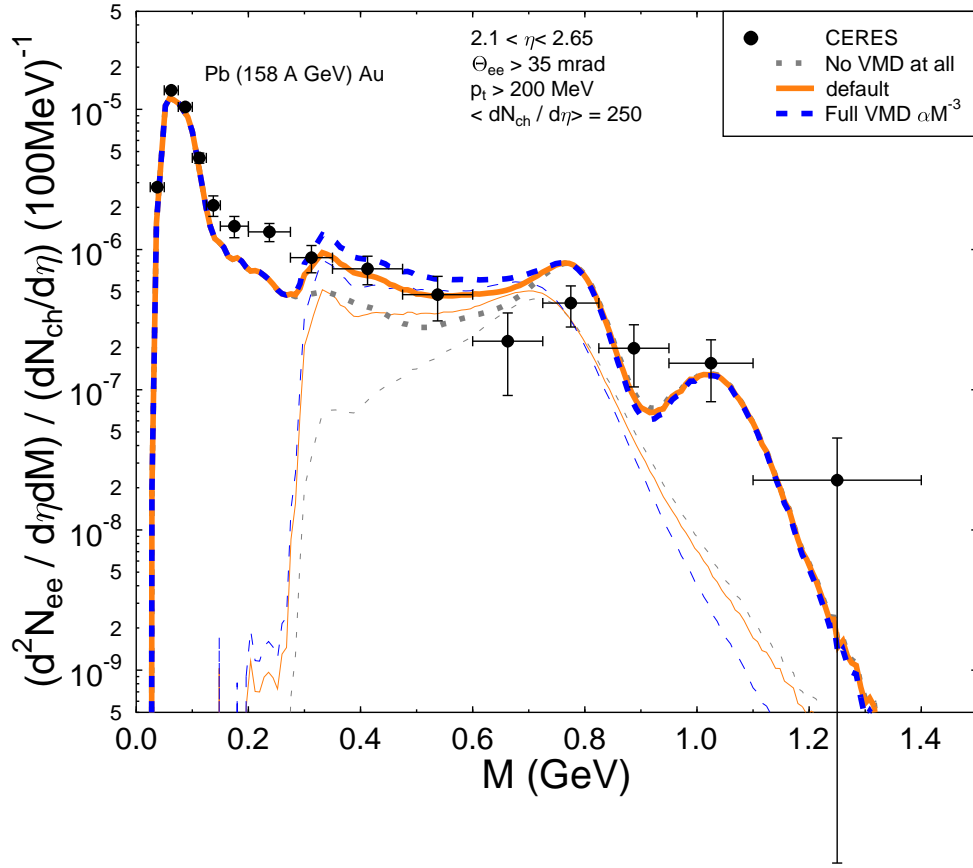


**Fig. 4** Effect of the mass dependence of the  $\rho$  meson dilepton decay width. Thin lines represent the mass distributions in the  $\rho$  channel while fat lines are the total spectra. (See text for more details.)

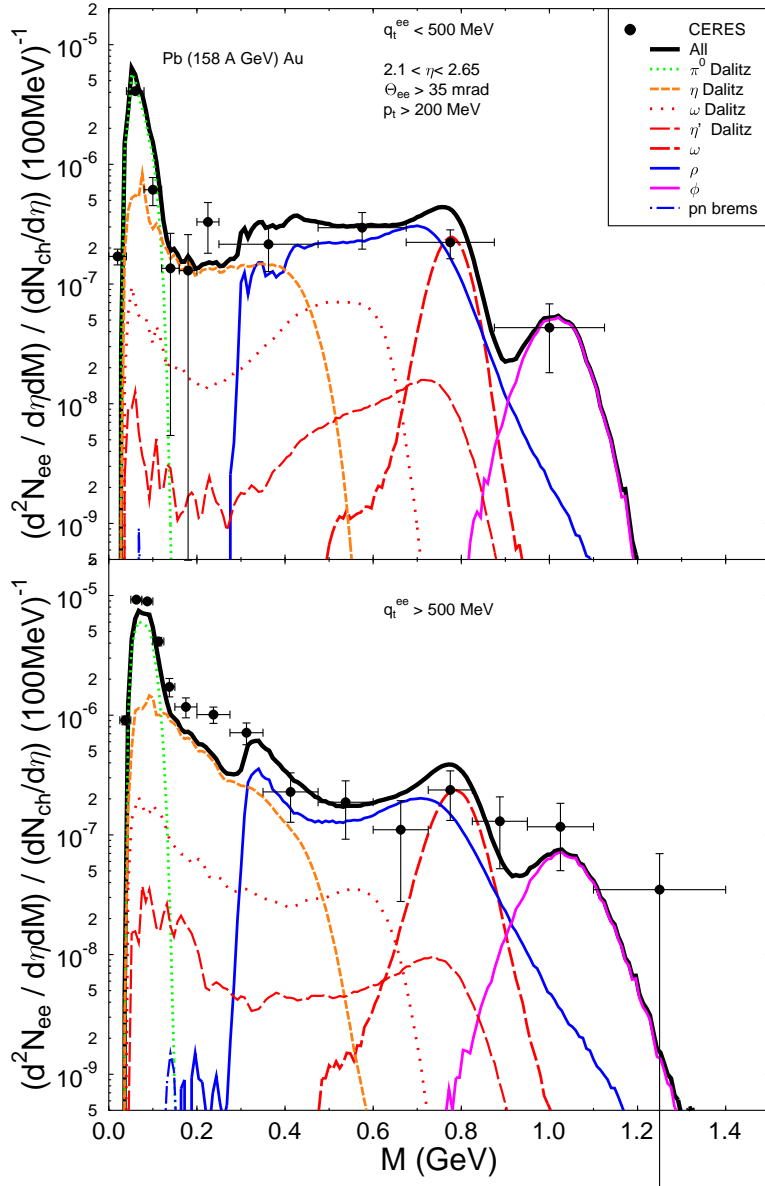


**Fig. 5** Same as fig. 3 but with additional cuts on the pair transverse momentum  $q_t^{e^+e^-}$  of the dilepton. The low  $p_t$  set is displayed in the upper part.